

Study of high momentum η' production in $B \rightarrow \eta' X_s$

B. Aubert,¹ R. Barate,¹ D. Boutigny,¹ F. Couderc,¹ J.-M. Gaillard,¹ A. Hicheur,¹ Y. Karyotakis,¹ J. P. Lees,¹ V. Tisserand,¹ A. Zghiche,¹ A. Palano,² A. Pompili,² J. C. Chen,³ N. D. Qi,³ G. Rong,³ P. Wang,³ Y. S. Zhu,³ G. Eigen,⁴ I. Ofte,⁴ B. Stugu,⁴ G. S. Abrams,⁵ A. W. Borgland,⁵ A. B. Breon,⁵ D. N. Brown,⁵ J. Button-Shafer,⁵ R. N. Cahn,⁵ E. Charles,⁵ C. T. Day,⁵ M. S. Gill,⁵ A. V. Gritsan,⁵ Y. Groysman,⁵ R. G. Jacobsen,⁵ R. W. Kadel,⁵ J. Kadyk,⁵ L. T. Kerth,⁵ Yu. G. Kolomensky,⁵ G. Kukartsev,⁵ C. LeClerc,⁵ M. E. Levi,⁵ G. Lynch,⁵ L. M. Mir,⁵ P. J. Oddone,⁵ T. J. Orimoto,⁵ M. Pripstein,⁵ N. A. Roe,⁵ M. T. Ronan,⁵ V. G. Shelkov,⁵ A. V. Telnov,⁵ W. A. Wenzel,⁵ K. Ford,⁶ T. J. Harrison,⁶ C. M. Hawkes,⁶ S. E. Morgan,⁶ A. T. Watson,⁶ N. K. Watson,⁶ M. Fritsch,⁷ K. Goetzen,⁷ T. Held,⁷ H. Koch,⁷ B. Lewandowski,⁷ M. Pelizaeus,⁷ K. Peters,⁷ H. Schmuecker,⁷ M. Steinke,⁷ J. T. Boyd,⁸ N. Chevalier,⁸ W. N. Cottingham,⁸ M. P. Kelly,⁸ T. E. Latham,⁸ C. Mackay,⁸ F. F. Wilson,⁸ K. Abe,⁹ T. Cuhadar-Donszelmann,⁹ C. Hearty,⁹ T. S. Mattison,⁹ J. A. McKenna,⁹ D. Thiessen,⁹ P. Kyberd,¹⁰ A. K. McKemey,¹⁰ L. Teodorescu,¹⁰ V. E. Blinov,¹¹ A. D. Bukin,¹¹ V. B. Golubev,¹¹ V. N. Ivanchenko,¹¹ E. A. Kravchenko,¹¹ A. P. Onuchin,¹¹ S. I. Serednyakov,¹¹ Yu. I. Skovpen,¹¹ E. P. Solodov,¹¹ A. N. Yushkov,¹¹ D. Best,¹² M. Bruinsma,¹² M. Chao,¹² I. Eschrich,¹² D. Kirkby,¹² A. J. Lankford,¹² M. Mandelkern,¹² R. K. Mommsen,¹² W. Roethel,¹² D. P. Stoker,¹² C. Buchanan,¹³ B. L. Hartfiel,¹³ J. W. Gary,¹⁴ J. Layter,¹⁴ B. C. Shen,¹⁴ K. Wang,¹⁴ D. del Re,¹⁵ H. K. Hadavand,¹⁵ E. J. Hill,¹⁵ D. B. MacFarlane,¹⁵ H. P. Paar,¹⁵ Sh. Rahatlou,¹⁵ V. Sharma,¹⁵ J. W. Berryhill,¹⁶ C. Campagnari,¹⁶ B. Dahmes,¹⁶ S. L. Levy,¹⁶ O. Long,¹⁶ A. Lu,¹⁶ M. A. Mazur,¹⁶ J. D. Richman,¹⁶ W. Verkerke,¹⁶ T. W. Beck,¹⁷ J. Beringer,¹⁷ A. M. Eisner,¹⁷ C. A. Heusch,¹⁷ W. S. Lockman,¹⁷ T. Schalk,¹⁷ R. E. Schmitz,¹⁷ B. A. Schumm,¹⁷ A. Seiden,¹⁷ P. Spradlin,¹⁷ W. Walkowiak,¹⁷ D. C. Williams,¹⁷ M. G. Wilson,¹⁷ J. Albert,¹⁸ E. Chen,¹⁸ G. P. Dubois-Felsmann,¹⁸ A. Dvoretzki,¹⁸ R. J. Erwin,¹⁸ D. G. Hitlin,¹⁸ I. Narsky,¹⁸ T. Piatenko,¹⁸ F. C. Porter,¹⁸ A. Ryd,¹⁸ A. Samuel,¹⁸ S. Yang,¹⁸ S. Jayatilake,¹⁹ G. Mancinelli,¹⁹ B. T. Meadows,¹⁹ M. D. Sokoloff,¹⁹ T. Abe,²⁰ F. Blanc,²⁰ P. Bloom,²⁰ S. Chen,²⁰ P. J. Clark,²⁰ W. T. Ford,²⁰ U. Nauenberg,²⁰ A. Olivas,²⁰ P. Rankin,²⁰ J. Roy,²⁰ J. G. Smith,²⁰ W. C. van Hoek,²⁰ L. Zhang,²⁰ J. L. Harton,²¹ T. Hu,²¹ A. Soffer,²¹ W. H. Toki,²¹ R. J. Wilson,²¹ J. Zhang,²¹ D. Altenburg,²² T. Brandt,²² J. Brose,²² T. Colberg,²² M. Dickopp,²² E. Feltresi,²² A. Hauke,²² H. M. Lacker,²² E. Maly,²² R. Müller-Pfefferkorn,²² R. Nogowski,²² S. Otto,²² J. Schubert,²² K. R. Schubert,²² R. Schwierz,²² B. Spaan,²² D. Bernard,²³ G. R. Bonneaud,²³ F. Brochard,²³ P. Grenier,²³ Ch. Thiebaut,²³ G. Vasileiadis,²³ M. Verderi,²³ D. J. Bard,²⁴ A. Khan,²⁴ D. Lavin,²⁴ F. Muheim,²⁴ S. Playfer,²⁴ M. Andreotti,²⁵ V. Azzolini,²⁵ D. Bettoni,²⁵ C. Bozzi,²⁵ R. Calabrese,²⁵ G. Cibinetto,²⁵ E. Luppi,²⁵ M. Negrini,²⁵ L. Piemontese,²⁵ A. Sarti,²⁵ E. Treadwell,²⁶ R. Baldini-Ferroli,²⁷ A. Calcaterra,²⁷ R. de Sangro,²⁷ G. Finocchiaro,²⁷ P. Patteri,²⁷ M. Piccolo,²⁷ A. Zallo,²⁷ A. Buzzo,²⁸ R. Capra,²⁸ R. Contri,²⁸ G. Crosetti,²⁸ M. Lo Vetere,²⁸ M. Macri,²⁸ M. R. Monge,²⁸ S. Passaggio,²⁸ C. Patrignani,²⁸ E. Robutti,²⁸ A. Santroni,²⁸ S. Tosi,²⁸ S. Bailey,²⁹ M. Morii,²⁹ E. Won,²⁹ R. S. Dubitzky,³⁰ U. Langenegger,³⁰ W. Bhimji,³¹ D. A. Bowerman,³¹ P. D. Dauncey,³¹ U. Egede,³¹ J. R. Gaillard,³¹ G. W. Morton,³¹ J. A. Nash,³¹ G. P. Taylor,³¹ G. J. Grenier,³² S.-J. Lee,³² U. Mallik,³² J. Cochran,³³ H. B. Crawley,³³ J. Lamsa,³³ W. T. Meyer,³³ S. Prell,³³ E. I. Rosenberg,³³ J. Yi,³³ M. Davier,³⁴ G. Grosdidier,³⁴ A. Höcker,³⁴ S. Laplace,³⁴ F. Le Diberder,³⁴ V. Lepeltier,³⁴ A. M. Lutz,³⁴ T. C. Petersen,³⁴ S. Plaszczynski,³⁴ M. H. Schune,³⁴ L. Tantot,³⁴ G. Wormser,³⁴ V. Brigljević,³⁵ C. H. Cheng,³⁵ D. J. Lange,³⁵ M. C. Simani,³⁵ D. M. Wright,³⁵ A. J. Bevan,³⁶ J. P. Coleman,³⁶ J. R. Fry,³⁶ E. Gabathuler,³⁶ R. Gamet,³⁶ M. Kay,³⁶ R. J. Parry,³⁶ D. J. Payne,³⁶ R. J. Sloane,³⁶ C. Touramanis,³⁶ J. J. Back,³⁷ P. F. Harrison,³⁷ G. B. Mohanty,³⁷ C. L. Brown,³⁸ G. Cowan,³⁸ R. L. Flack,³⁸ H. U. Flaecher,³⁸ S. George,³⁸ M. G. Green,³⁸ A. Kurup,³⁸ C. E. Marker,³⁸ T. R. McMahon,³⁸ S. Ricciardi,³⁸ F. Salvatore,³⁸ G. Vaitsas,³⁸ M. A. Winter,³⁸ D. Brown,³⁹ C. L. Davis,³⁹ J. Allison,⁴⁰ N. R. Barlow,⁴⁰ R. J. Barlow,⁴⁰ P. A. Hart,⁴⁰ M. C. Hodgkinson,⁴⁰ G. D. Lafferty,⁴⁰ A. J. Lyon,⁴⁰ J. C. Williams,⁴⁰ A. Farbin,⁴¹ W. D. Hulsbergen,⁴¹ A. Jawahery,⁴¹ D. Kovalskyi,⁴¹ C. K. Lae,⁴¹ V. Lillard,⁴¹ D. A. Roberts,⁴¹ G. Blaylock,⁴² C. Dallapiccola,⁴² K. T. Flood,⁴² S. S. Hertzbach,⁴² R. Kofler,⁴² V. B. Koptchev,⁴² T. B. Moore,⁴² S. Saremi,⁴² H. Staengle,⁴² S. Willocq,⁴² R. Cowan,⁴³ G. Sciolla,⁴³ F. Taylor,⁴³ R. K. Yamamoto,⁴³ D. J. J. Mangeol,⁴⁴ P. M. Patel,⁴⁴ S. H. Robertson,⁴⁴ A. Lazzaro,⁴⁵ F. Palombo,⁴⁵ J. M. Bauer,⁴⁶ L. Cremaldi,⁴⁶ V. Eschenburg,⁴⁶ R. Godang,⁴⁶ R. Kroeger,⁴⁶ J. Reidy,⁴⁶ D. A. Sanders,⁴⁶

D. J. Summers,⁴⁶ H. W. Zhao,⁴⁶ S. Brunet,⁴⁷ D. Cote-Ahern,⁴⁷ P. Taras,⁴⁷ H. Nicholson,⁴⁸ C. Cartaro,⁴⁹ N. Cavallo,⁴⁹ G. De Nardo,⁴⁹ F. Fabozzi,^{49,*} C. Gatto,⁴⁹ L. Lista,⁴⁹ P. Paolucci,⁴⁹ D. Piccolo,⁴⁹ C. Sciacca,⁴⁹ M. A. Baak,⁵⁰ G. Raven,⁵⁰ L. Wilden,⁵⁰ C. P. Jessop,⁵¹ J. M. LoSecco,⁵¹ T. A. Gabriel,⁵² T. Allmendinger,⁵³ B. Brau,⁵³ K. K. Gan,⁵³ K. Honscheid,⁵³ D. Hufnagel,⁵³ H. Kagan,⁵³ R. Kass,⁵³ T. Pulliam,⁵³ R. Ter-Antonyan,⁵³ Q. K. Wong,⁵³ J. Brau,⁵⁴ R. Frey,⁵⁴ O. Igonkina,⁵⁴ C. T. Potter,⁵⁴ N. B. Sinev,⁵⁴ D. Strom,⁵⁴ E. Torrence,⁵⁴ F. Colechia,⁵⁵ A. Dorigo,⁵⁵ F. Galeazzi,⁵⁵ M. Margoni,⁵⁵ M. Morandin,⁵⁵ M. Posocco,⁵⁵ M. Rotondo,⁵⁵ F. Simonetto,⁵⁵ R. Stroili,⁵⁵ G. Tiozzo,⁵⁵ C. Voci,⁵⁵ M. Benayoun,⁵⁶ H. Briand,⁵⁶ J. Chauveau,⁵⁶ P. David,⁵⁶ Ch. de la Vaissière,⁵⁶ L. Del Buono,⁵⁶ O. Hamon,⁵⁶ M. J. J. John,⁵⁶ Ph. Leruste,⁵⁶ J. Ocariz,⁵⁶ M. Pivk,⁵⁶ L. Roos,⁵⁶ S. T'Jampens,⁵⁶ G. Therin,⁵⁶ P. F. Manfredi,⁵⁷ V. Re,⁵⁷ P. K. Behera,⁵⁸ L. Gladney,⁵⁸ Q. H. Guo,⁵⁸ J. Panetta,⁵⁸ F. Anulli,^{27,59} M. Biasini,⁵⁹ I. M. Peruzzi,^{27,59} M. Pioppi,⁵⁹ C. Angelini,⁶⁰ G. Batignani,⁶⁰ S. Bettarini,⁶⁰ M. Bondioli,⁶⁰ F. Bucci,⁶⁰ G. Calderini,⁶⁰ M. Carpinelli,⁶⁰ V. Del Gamba,⁶⁰ F. Forti,⁶⁰ M. A. Giorgi,⁶⁰ A. Lusiani,⁶⁰ G. Marchiori,⁶⁰ F. Martinez-Vidal,^{60,†} M. Morganti,⁶⁰ N. Neri,⁶⁰ E. Paoloni,⁶⁰ M. Rama,⁶⁰ G. Rizzo,⁶⁰ F. Sandrelli,⁶⁰ J. Walsh,⁶⁰ M. Haire,⁶¹ D. Judd,⁶¹ K. Paick,⁶¹ D. E. Wagoner,⁶¹ N. Danielson,⁶² P. Elmer,⁶² C. Lu,⁶² V. Miftakov,⁶² J. Olsen,⁶² A. J. S. Smith,⁶² E. W. Varnes,⁶² F. Bellini,⁶³ G. Cavoto,^{62,63} R. Faccini,⁶³ F. Ferrarotto,⁶³ F. Ferroni,⁶³ M. Gaspero,⁶³ M. A. Mazzone,⁶³ S. Morganti,⁶³ M. Pierini,⁶³ G. Piredda,⁶³ F. Safai Tehrani,⁶³ C. Voena,⁶³ S. Christ,⁶⁴ G. Wagner,⁶⁴ R. Waldi,⁶⁴ T. Adye,⁶⁵ N. De Groot,⁶⁵ B. Franek,⁶⁵ N. I. Geddes,⁶⁵ G. P. Gopal,⁶⁵ E. O. Olaiya,⁶⁵ S. M. Xella,⁶⁵ R. Aleksan,⁶⁶ S. Emery,⁶⁶ A. Gaidot,⁶⁶ S. F. Ganzhur,⁶⁶ P.-F. Giraud,⁶⁶ G. Hamel de Monchenault,⁶⁶ W. Kozanecki,⁶⁶ M. Langer,⁶⁶ M. Legendre,⁶⁶ G. W. London,⁶⁶ B. Mayer,⁶⁶ G. Schott,⁶⁶ G. Vasseur,⁶⁶ Ch. Yeche,⁶⁶ M. Zito,⁶⁶ M. V. Purohit,⁶⁷ A. W. Weidemann,⁶⁷ F. X. Yumiceva,⁶⁷ D. Aston,⁶⁸ R. Bartoldus,⁶⁸ N. Berger,⁶⁸ A. M. Boyarski,⁶⁸ O. L. Buchmueller,⁶⁸ M. R. Convery,⁶⁸ M. Cristinziani,⁶⁸ D. Dong,⁶⁸ J. Dorfan,⁶⁸ D. Dujmic,⁶⁸ W. Dunwoodie,⁶⁸ E. E. Elsen,⁶⁸ R. C. Field,⁶⁸ T. Glanzman,⁶⁸ S. J. Gowdy,⁶⁸ T. Hadig,⁶⁸ V. Halyo,⁶⁸ T. Hryn'ova,⁶⁸ W. R. Innes,⁶⁸ M. H. Kelsey,⁶⁸ P. Kim,⁶⁸ M. L. Kocian,⁶⁸ D. W. G. S. Leith,⁶⁸ J. Libby,⁶⁸ S. Luitz,⁶⁸ V. Luth,⁶⁸ H. L. Lynch,⁶⁸ H. Marsiske,⁶⁸ R. Messner,⁶⁸ D. R. Muller,⁶⁸ C. P. O'Grady,⁶⁸ V. E. Ozcan,⁶⁸ A. Perazzo,⁶⁸ M. Perl,⁶⁸ S. Petrak,⁶⁸ B. N. Ratcliff,⁶⁸ A. Roodman,⁶⁸ A. A. Salnikov,⁶⁸ R. H. Schindler,⁶⁸ J. Schwiening,⁶⁸ G. Simi,⁶⁸ A. Snyder,⁶⁸ A. Soha,⁶⁸ J. Stelzer,⁶⁸ D. Su,⁶⁸ M. K. Sullivan,⁶⁸ J. Va'vra,⁶⁸ S. R. Wagner,⁶⁸ M. Weaver,⁶⁸ A. J. R. Weinstein,⁶⁸ W. J. Wisniewski,⁶⁸ D. H. Wright,⁶⁸ C. C. Young,⁶⁸ P. R. Burchat,⁶⁹ A. J. Edwards,⁶⁹ T. I. Meyer,⁶⁹ B. A. Petersen,⁶⁹ C. Roat,⁶⁹ M. Ahmed,⁷⁰ S. Ahmed,⁷⁰ M. S. Alam,⁷⁰ J. A. Ernst,⁷⁰ M. A. Saeed,⁷⁰ M. Saleem,⁷⁰ F. R. Wappler,⁷⁰ W. Bugg,⁷¹ M. Krishnamurthy,⁷¹ S. M. Spanier,⁷¹ R. Eckmann,⁷² H. Kim,⁷² J. L. Ritchie,⁷² A. Satpathy,⁷² R. F. Schwitters,⁷² J. M. Izen,⁷³ I. Kitayama,⁷³ X. C. Lou,⁷³ S. Ye,⁷³ F. Bianchi,⁷⁴ M. Bona,⁷⁴ F. Gallo,⁷⁴ D. Gamba,⁷⁴ C. Borean,⁷⁵ L. Bosisio,⁷⁵ F. Cossutti,⁷⁵ G. Della Ricca,⁷⁵ S. Dittongo,⁷⁵ S. Grancagnolo,⁷⁵ L. Lancieri,⁷⁵ P. Poropat,^{75,‡} L. Vitale,⁷⁵ G. Vuagnin,⁷⁵ R. S. Panvini,⁷⁶ Sw. Banerjee,⁷⁷ C. M. Brown,⁷⁷ D. Fortin,⁷⁷ P. D. Jackson,⁷⁷ R. Kowalewski,⁷⁷ J. M. Roney,⁷⁷ H. R. Band,⁷⁸ S. Dasu,⁷⁸ M. Datta,⁷⁸ A. M. Eichenbaum,⁷⁸ J. R. Johnson,⁷⁸ P. E. Kutter,⁷⁸ H. Li,⁷⁸ R. Liu,⁷⁸ F. Di Lodovico,⁷⁸ A. Mihalyi,⁷⁸ A. K. Mohapatra,⁷⁸ Y. Pan,⁷⁸ R. Prepost,⁷⁸ S. J. Sekula,⁷⁸ J. H. von Wimmersperg-Toeller,⁷⁸ J. Wu,⁷⁸ S. L. Wu,⁷⁸ Z. Yu,⁷⁸ and H. Neal⁷⁹

(The BABAR Collaboration)

¹Laboratoire de Physique des Particules, F-74941 Annecy-le-Vieux, France

²Università di Bari, Dipartimento di Fisica and INFN, I-70126 Bari, Italy

³Institute of High Energy Physics, Beijing 100039, China

⁴University of Bergen, Inst. of Physics, N-5007 Bergen, Norway

⁵Lawrence Berkeley National Laboratory and University of California, Berkeley, CA 94720, USA

⁶University of Birmingham, Birmingham, B15 2TT, United Kingdom

⁷Ruhr Universität Bochum, Institut für Experimentalphysik 1, D-44780 Bochum, Germany

⁸University of Bristol, Bristol BS8 1TL, United Kingdom

⁹University of British Columbia, Vancouver, BC, Canada V6T 1Z1

¹⁰Brunel University, Uxbridge, Middlesex UB8 3PH, United Kingdom

¹¹Budker Institute of Nuclear Physics, Novosibirsk 630090, Russia

¹²University of California at Irvine, Irvine, CA 92697, USA

¹³University of California at Los Angeles, Los Angeles, CA 90024, USA

¹⁴University of California at Riverside, Riverside, CA 92521, USA

¹⁵University of California at San Diego, La Jolla, CA 92093, USA

¹⁶University of California at Santa Barbara, Santa Barbara, CA 93106, USA

¹⁷University of California at Santa Cruz, Institute for Particle Physics, Santa Cruz, CA 95064, USA

¹⁸California Institute of Technology, Pasadena, CA 91125, USA

¹⁹University of Cincinnati, Cincinnati, OH 45221, USA

- ²⁰ University of Colorado, Boulder, CO 80309, USA
- ²¹ Colorado State University, Fort Collins, CO 80523, USA
- ²² Technische Universität Dresden, Institut für Kern- und Teilchenphysik, D-01062 Dresden, Germany
- ²³ Ecole Polytechnique, LLR, F-91128 Palaiseau, France
- ²⁴ University of Edinburgh, Edinburgh EH9 3JZ, United Kingdom
- ²⁵ Università di Ferrara, Dipartimento di Fisica and INFN, I-44100 Ferrara, Italy
- ²⁶ Florida A&M University, Tallahassee, FL 32307, USA
- ²⁷ Laboratori Nazionali di Frascati dell'INFN, I-00044 Frascati, Italy
- ²⁸ Università di Genova, Dipartimento di Fisica and INFN, I-16146 Genova, Italy
- ²⁹ Harvard University, Cambridge, MA 02138, USA
- ³⁰ Universität Heidelberg, Physikalisches Institut, Philosophenweg 12, D-69120 Heidelberg, Germany
- ³¹ Imperial College London, London, SW7 2AZ, United Kingdom
- ³² University of Iowa, Iowa City, IA 52242, USA
- ³³ Iowa State University, Ames, IA 50011-3160, USA
- ³⁴ Laboratoire de l'Accélérateur Linéaire, F-91898 Orsay, France
- ³⁵ Lawrence Livermore National Laboratory, Livermore, CA 94550, USA
- ³⁶ University of Liverpool, Liverpool L69 3BX, United Kingdom
- ³⁷ Queen Mary, University of London, E1 4NS, United Kingdom
- ³⁸ University of London, Royal Holloway and Bedford New College, Egham, Surrey TW20 0EX, United Kingdom
- ³⁹ University of Louisville, Louisville, KY 40292, USA
- ⁴⁰ University of Manchester, Manchester M13 9PL, United Kingdom
- ⁴¹ University of Maryland, College Park, MD 20742, USA
- ⁴² University of Massachusetts, Amherst, MA 01003, USA
- ⁴³ Massachusetts Institute of Technology, Laboratory for Nuclear Science, Cambridge, MA 02139, USA
- ⁴⁴ McGill University, Montréal, QC, Canada H3A 2T8
- ⁴⁵ Università di Milano, Dipartimento di Fisica and INFN, I-20133 Milano, Italy
- ⁴⁶ University of Mississippi, University, MS 38677, USA
- ⁴⁷ Université de Montréal, Laboratoire René J. A. Lévesque, Montréal, QC, Canada H3C 3J7
- ⁴⁸ Mount Holyoke College, South Hadley, MA 01075, USA
- ⁴⁹ Università di Napoli Federico II, Dipartimento di Scienze Fisiche and INFN, I-80126, Napoli, Italy
- ⁵⁰ NIKHEF, National Institute for Nuclear Physics and High Energy Physics, NL-1009 DB Amsterdam, The Netherlands
- ⁵¹ University of Notre Dame, Notre Dame, IN 46556, USA
- ⁵² Oak Ridge National Laboratory, Oak Ridge, TN 37831, USA
- ⁵³ Ohio State University, Columbus, OH 43210, USA
- ⁵⁴ University of Oregon, Eugene, OR 97403, USA
- ⁵⁵ Università di Padova, Dipartimento di Fisica and INFN, I-35131 Padova, Italy
- ⁵⁶ Universités Paris VI et VII, Lab de Physique Nucléaire H. E., F-75252 Paris, France
- ⁵⁷ Università di Pavia, Dipartimento di Elettronica and INFN, I-27100 Pavia, Italy
- ⁵⁸ University of Pennsylvania, Philadelphia, PA 19104, USA
- ⁵⁹ Università di Perugia, Dipartimento di Fisica and INFN, I-06100 Perugia, Italy
- ⁶⁰ Università di Pisa, Dipartimento di Fisica, Scuola Normale Superiore and INFN, I-56127 Pisa, Italy
- ⁶¹ Prairie View A&M University, Prairie View, TX 77446, USA
- ⁶² Princeton University, Princeton, NJ 08544, USA
- ⁶³ Università di Roma La Sapienza, Dipartimento di Fisica and INFN, I-00185 Roma, Italy
- ⁶⁴ Universität Rostock, D-18051 Rostock, Germany
- ⁶⁵ Rutherford Appleton Laboratory, Chilton, Didcot, Oxon, OX11 0QX, United Kingdom
- ⁶⁶ DSM/Dapnia, CEA/Saclay, F-91191 Gif-sur-Yvette, France
- ⁶⁷ University of South Carolina, Columbia, SC 29208, USA
- ⁶⁸ Stanford Linear Accelerator Center, Stanford, CA 94309, USA
- ⁶⁹ Stanford University, Stanford, CA 94305-4060, USA
- ⁷⁰ State Univ. of New York, Albany, NY 12222, USA
- ⁷¹ University of Tennessee, Knoxville, TN 37996, USA
- ⁷² University of Texas at Austin, Austin, TX 78712, USA
- ⁷³ University of Texas at Dallas, Richardson, TX 75083, USA
- ⁷⁴ Università di Torino, Dipartimento di Fisica Sperimentale and INFN, I-10125 Torino, Italy
- ⁷⁵ Università di Trieste, Dipartimento di Fisica and INFN, I-34127 Trieste, Italy
- ⁷⁶ Vanderbilt University, Nashville, TN 37235, USA
- ⁷⁷ University of Victoria, Victoria, BC, Canada V8W 3P6
- ⁷⁸ University of Wisconsin, Madison, WI 53706, USA
- ⁷⁹ Yale University, New Haven, CT 06511, USA

We measure the branching fraction for the charmless semi-inclusive process $B \rightarrow \eta' X_s$, where the η' meson has a momentum in the range 2.0 to 2.7 GeV/c in the $\Upsilon(4S)$ center-of-mass frame and X_s represents a system comprising a kaon and zero to four pions. We find $\mathcal{B}(B \rightarrow \eta' X_s) =$

$(3.9 \pm 0.8(\text{stat}) \pm 0.5(\text{syst}) \pm 0.8(\text{model})) \times 10^{-4}$. We also obtain the X_s mass distribution and find that it tends to favor models predicting high masses.

The production of high momentum η' mesons in B meson decays is expected to be dominated by the $B \rightarrow \eta' X_s$ process, where X_s is a strange hadronic system, generated by the $b \rightarrow sg^*$ transition as depicted in Fig. 1(a-c). Figure 1(d) shows the color-suppressed modes $\bar{B}^0 \rightarrow \eta' D^{(*)0}$, which are significant sources of background and which have been measured for the first time recently [1]. Contributions from $b \rightarrow u$ transitions and other sources of η' are expected to be negligible [2].

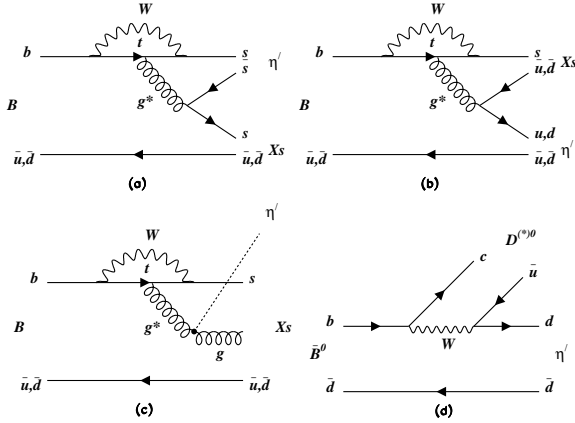


FIG. 1: Lowest order diagrams for (a,b,c) $B \rightarrow \eta' X_s$ and (d) the color-suppressed background $\bar{B}^0 \rightarrow \eta' D^{(*)0}$.

The large $B \rightarrow \eta' X_s$ branching fraction measured by the CLEO collaboration [3], prompted intense theoretical activity, which focused the special character of the η' meson as receiving much of its mass from the QCD anomaly.

A later measurement by CLEO confirmed the large η' production, measuring $\mathcal{B}(B \rightarrow \eta' X_{nc}) = (4.6 \pm 1.1(\text{stat}) \pm 0.4(\text{syst}) \pm 0.5(\text{bkg})) \times 10^{-4}$ [8], where X_{nc} denotes a charmless recoiling hadronic system.

The rate for $B \rightarrow \eta' X_s$ and especially the fully background-subtracted distribution of the mass of X_s can provide important clues to the dynamics of weak decays and to the structure of the isosinglet pseudoscalar mesons.

We present results for the branching fraction $\mathcal{B}(B \rightarrow \eta' X_s)$ and the mass spectrum of X_s . The signal is analyzed for η' momentum between 2.0 and 2.7 GeV/c in the CM to suppress background coming from $b \rightarrow c \rightarrow \eta'$ cascades such as $B \rightarrow D_s X$ with $D_s \rightarrow \eta' X$, $B \rightarrow DX$ with $D \rightarrow \eta' X$, $B \rightarrow A_c X$ with $A_c \rightarrow \eta' X$. Our analysis is based on data collected with the BABAR detector [9] at the PEP-II asymmetric e^+e^- collider located at the Stanford Linear Accelerator Center. An integrated luminosity of 81.4 fb^{-1} , corresponding to 88.4 million $B\bar{B}$ pairs, was recorded at the $\Upsilon(4S)$ resonance (on-resonance) and 9.6

fb^{-1} were recorded 40 MeV below this resonance (off-resonance), for continuum background studies.

Two tracking devices are used for the detection of charged particles: a silicon vertex tracker consisting of five layers of double-sided silicon microstrip detectors, and a 40-layer central drift chamber, both operating in the 1.5 T magnetic field of a superconducting solenoid. Photons and electrons are detected by a CsI(Tl) electromagnetic calorimeter. Charged-particle identification is provided by the average energy loss (dE/dx) in the tracking devices, and by an internally reflecting ring-imaging Cherenkov detector covering the central region.

We select $B\bar{B}$ events by requiring at least four charged tracks and a value of the ratio of the second to zeroth Fox-Wolfram moment [10] less than 0.5.

We form a B candidate by combining an $\eta' \rightarrow \eta\pi^+\pi^-$, where the η decays into $\gamma\gamma$, with a K^+ or a K_s^0 that is reconstructed in the $\pi^+\pi^-$ channel, and up to four pions, of which at most one is a π^0 , leading to 16 possible channels [11]:

$$\begin{aligned} B^+ &\rightarrow \eta' K^+ (+\pi^0) & B^0 &\rightarrow \eta' K_s^0 (+\pi^0) \\ B^+ &\rightarrow \eta' K^+ \pi^+ \pi^- (+\pi^0) & B^0 &\rightarrow \eta' K_s^0 \pi^+ \pi^- (+\pi^0) \\ B^+ &\rightarrow \eta' K_s^0 \pi^+ (+\pi^0) & B^0 &\rightarrow \eta' K^+ \pi^- (+\pi^0) \\ B^+ &\rightarrow \eta' K_s^0 \pi^+ \pi^+ \pi^- (+\pi^0) & B^0 &\rightarrow \eta' K^+ \pi^- \pi^+ \pi^- (+\pi^0) \end{aligned}$$

The mass of the $\eta \rightarrow \gamma\gamma$, $K_s^0 \rightarrow \pi^+\pi^-$ and $\pi^0 \rightarrow \gamma\gamma$ candidates are required to lie within 3σ ($\sigma = 16, 3$ and $6 \text{ MeV}/c^2$ respectively) of their known values and are then kinematically constrained to their nominal masses.

To identify the s quark in the X_s system, we require a K_s^0 or a track consistent with a charged kaon. The charged-kaon selection has been optimized to reduce background from $B \rightarrow \eta'\pi$, $\eta'\rho$, and $\eta'a_1$ decays. For the K_s^0 , we require the angle α between the momentum of the K_s^0 candidate and its flight direction to be less than 0.05 radians, as it peaks at zero for true K_s^0 particles.

We require candidates for $B \rightarrow \eta' X_s$ to be consistent with a B decay, based on the beam-energy-substituted mass, $m_{\text{ES}} = \sqrt{(s/2 + \mathbf{p}_0 \cdot \mathbf{p}_B)^2 / E_0^2 - \mathbf{p}_B^2}$ and the energy difference, $\Delta E = E_B^* - \sqrt{s}/2$, where E and \mathbf{p} denote the energy and momentum of the particles, the subscripts 0 and B refer to the initial $\Upsilon(4S)$ and the B candidate, respectively, the asterisk denotes the $\Upsilon(4S)$ rest frame, and \sqrt{s} is the e^+e^- center-of-mass energy. In addition, the cosine of the angle between the thrust axis of the B candidate and that of the rest of the event in the center-of-mass frame ($\cos\theta_T^*$) is used to remove continuum background, which is peaked near $|\cos\theta_T^*| = 1$, while signal events are uniformly distributed. We require $m_{\text{ES}} > 5.265 \text{ GeV}/c^2$, $|\Delta E| < 0.1 \text{ GeV}$, and $|\cos\theta_T^*| < 0.8$. For each event, we select the candidate with the smallest χ^2 , with χ^2 defined by

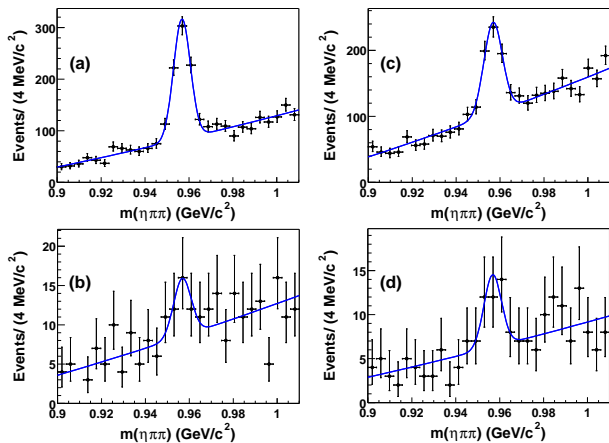


FIG. 2: Fits to the $\eta\pi\pi$ invariant mass for on-resonance (top) and off-resonance (bottom) data samples, for the modes (a,b) K^\pm and (c,d) K_s^0 .

$$\chi^2 = (m_{\text{ES}} - M_B)^2/\sigma^2(m_{\text{ES}}) + (\Delta E)^2/\sigma^2(\Delta E),$$

where M_B is the B -meson mass and where the resolutions $\sigma(m_{\text{ES}}) = 3 \text{ MeV}/c^2$ and $\sigma(\Delta E) = 25 \text{ MeV}$ are obtained from Monte Carlo simulation. The remaining continuum background is subtracted with the use of off-resonance data.

The background contribution from color-suppressed modes $\bar{B}^0 \rightarrow \eta' D^{(*)0}$ is estimated from a Monte Carlo simulation which uses our measurement of its branching fraction, $\mathcal{B}(\bar{B}^0 \rightarrow \eta' D^{(*)0}) = (1.7 \pm 0.4(\text{stat}) \pm 0.2(\text{syst})) \times 10^{-4}$ [1].

To determine efficiencies, we model the signal using a combination of the two-body mode $B \rightarrow \eta' K$ and, for X_s masses above the $K\pi$ threshold, a non-resonant derived from the theoretical predictions [4, 5, 6], which are based on the anomalous η' -gluon-gluon coupling and which favor high-mass X_s systems. The fraction of the two-body mode is constrained in the simulation model to be between 10% and 15% [13, 14]. When not forming a K meson, the X_s fragments into $s\bar{q}$ and $s\bar{q}g$ ($q = u, d$). We find that the overall efficiency is $(6.0 \pm 0.2)\%$ for the K^\pm modes and $(4.7 \pm 0.1)\%$ for the K_s^0 modes, including the branching fraction $\mathcal{B}(K_s^0 \rightarrow \pi^+\pi^-)$.

The branching fraction of $B \rightarrow \eta' X_s$ is computed through a fit to the number of η' signal events, with η' momentum between 2.0 and 2.7 GeV/c , both for on-resonance and off-resonance data. To parameterize the background, we use a Gaussian function for the signal and a second order polynomial. For the fit of the off-resonance data sample, we constrain the mass and width of the η' to the values obtained with on-resonance data. Figure 2 shows the fits of the $\eta\pi\pi$ invariant mass distributions for the K^\pm and K_s^0 modes. The fitted yields are reported in Table I.

The semi-inclusive branching fraction is computed by

TABLE I: Results of the fits for K^\pm and K_s^0 modes. Yields for on-resonance data (Y_{ON}), off-resonance data (Y_{OFF}), expectation from color-suppressed background (Y_{CS}) and on-resonance data after background subtraction (Y) are given. A luminosity scale factor, $f = 8.48$, is applied to the off-resonance yield.

	K^\pm modes	K_s^0 modes
Y_{ON}	577.0 ± 34.0	367.0 ± 34.0
Y_{OFF}	18.9 ± 8.5	21.7 ± 8.4
Y_{CS}	63.6 ± 11.4	26.9 ± 4.5
Y	353.1 ± 80.5	156.1 ± 79.1

TABLE II: Contribution of different sources to the systematic error for modes with a K^\pm or K_s^0 .

Source	K^\pm syst (%)	K_s^0 syst (%)
Tracking	3.4	3.3
η, π^0 detection	7.0	8.2
K/K_s^0 ID	2.5	4.3
$\mathcal{B}(\eta' \rightarrow \eta\gamma\pi\pi)$	3.4	3.4
$N_{B\bar{B}}$	1.1	1.1
MC sample size	3.0	3.0
$\eta' D^{(*)0}$ subtraction	3.0	2.9
Total	12.1	13.5
Model	20	20

performing a weighted average of the results obtained for the K^\pm and K_s^0 modes. The detection efficiencies are corrected to account for the η' and η branching fractions to the channel we observe. For the K_s^0 modes, we convert the result so it corresponds to K^0 and \bar{K}^0 . The final state X_s includes both K^+ - and K^0 -tagged decays. Assuming that their branching fractions are equal, we obtain $\mathcal{B}(B \rightarrow \eta' X_s) = (3.9 \pm 0.8(\text{stat}) \pm 0.5(\text{syst}) \pm 0.8(\text{model})) \times 10^{-4}$. We obtain the systematic error by combining the sources listed in Table II.

The largest uncertainty arises from our model of the X_s system. To estimate that uncertainty, we use an alternative model which consists of a combination of resonant modes: $\eta' K$, $\eta' K^*(892)$, $\eta' K_1(1270)$, $\eta' K_1(1400)$, $\eta' K^*(1410)$, $\eta' K_2^*(1430)$, $\eta' K_3^*(1780)$, and $\eta' K_4^*(2045)$. The variability of the efficiency and our knowledge of the resonant sector lead us to assign a 20% systematic uncertainty. Other systematic uncertainties include track reconstruction efficiency, reconstruction efficiencies of $\pi^0 \rightarrow \gamma\gamma$, $\eta \rightarrow \gamma\gamma$, and $K_s^0 \rightarrow \pi^+\pi^-$ candidates, charged-kaon identification efficiency, secondary branching fractions, number of $B\bar{B}$ events ($N_{B\bar{B}}$), the size of our Monte-Carlo sample, and subtraction of the background from $\bar{B}^0 \rightarrow \eta' D^{(*)0}$.

To explore the X_s mass distribution, we select B candidates for which the mass of the η' is within three standard deviations of the known value, and subtract the continuum contribution by using on-resonance data in the sideband $5.200 < m_{\text{ES}} < 5.265 \text{ GeV}/c^2$. The contin-

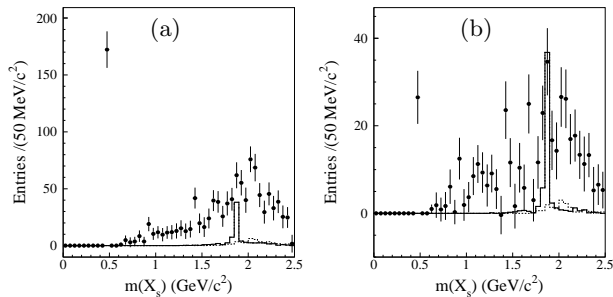


FIG. 3: Continuum-subtracted $K n \pi$ invariant-mass distributions for (a) all B modes and (b) B^0 modes, including combinatorial background. Solid and dashed histograms represent expected backgrounds from $\bar{B}^0 \rightarrow \eta' D^0$ and $\bar{B}^0 \rightarrow \eta' D^{*0}$, respectively.

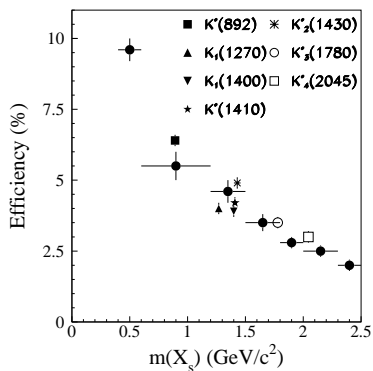


FIG. 4: Variation of efficiency with $m(X_s)$. The filled circles indicate the efficiency for non-resonant X_s simulation. The other symbols denote the values for the resonances.

uum background scaling factor (\mathcal{A}), from the sideband to signal regions, is computed from off-resonance data to be 0.591 ± 0.118 . The resulting mass distributions are shown in Fig. 3 for all B modes and separately for the B^0 modes. The peak at $m(X_s) \simeq 500 \text{ MeV}/c^2$ corresponds to the two body mode $B \rightarrow \eta' K$.

To obtain the full X_s spectrum, we fit the η' mass distribution in bins of X_s mass. The efficiency, averaged over the charged and neutral kaons, as a function of $m(X_s)$, is shown in Fig. 4. The correction for the feed-across between bins is included in the efficiencies.

According to simulations, the X_s system is correctly reconstructed for 85% (60%) of the candidates in the region $m(X_s) < 1.5 \text{ GeV}/c^2$ ($m(X_s) > 1.5 \text{ GeV}/c^2$). For correctly reconstructed events, the experimental resolution varies from 5 to 15 MeV/c^2 for low and high masses, respectively. In the case of misreconstructed events, the resolution ranges from 100 to 150 MeV/c^2 . Table III shows the fitted yields for the raw signal, the sideband region, the expected color-suppressed background, and the yield after full background subtraction, as a function

TABLE III: Fitted yields for on-resonance data and color-suppressed background for different $m(X_s)$ ranges in GeV/c^2 . The sideband yields (Y_{SB}) must be corrected by the sideband to signal region scaling factor (see text) before subtraction.

$m(X_s)$ range	Y_{ON}	Y_{SB}	Y_{CS}	Y
[0.4, 0.6]	200 ± 15	46.1 ± 8.8	—	172.8 ± 15.9
[0.6, 1.2]	120 ± 14	100 ± 13	—	60.9 ± 16.0
[1.2, 1.5]	114 ± 15	112 ± 14	1.1 ± 0.3	46.7 ± 17.1
[1.5, 1.8]	150 ± 18	163 ± 17	7.7 ± 1.6	46.0 ± 20.7
[1.8, 2.0]	140 ± 17	93 ± 15	47.4 ± 9.6	37.6 ± 21.4
[2.0, 2.3]	149 ± 20	142 ± 18	26.2 ± 4.5	38.9 ± 23.1
[2.3, 2.5]	80 ± 14	70 ± 14	4.9 ± 0.9	33.7 ± 16.3

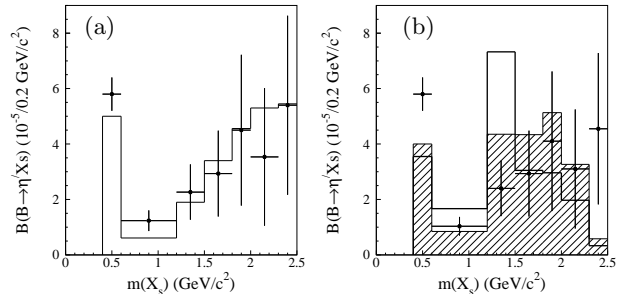


FIG. 5: Branching fractions as a function of $m(X_s)$. Both (a) and (b) show the same data, though the efficiency used in (a) is derived from the non-resonant model, while that in (b) the efficiency comes from the model with a combination of resonances. The errors include bin-to-bin systematics; an additional systematic error of $\sim 8\%$ (not shown) is common to all points. (a) The open histogram represents the expectation from non-resonant $m(X_s)$ simulation. (b) The open histogram represents the expectation from a mixture of resonant modes with equal proportions. The hatched histogram results if some heavy resonances are enhanced. The equal mixture provides a good approximation to what is predicted in [12].

of $m(X_s)$.

The branching fraction as a function of $m(X_s)$, obtained from the fully background-subtracted yield (Table III), is shown in Fig. 5.

We compare data and simulation by forming a χ^2 difference. The χ^2 probability for the nonresonant X_s model (Fig. 5(a)) to fit the data is 61% while it is close to $\sim 10^{-7}$ for the equal mixture of resonances (Fig. 5(b)). We find improved agreement with the resonant model if the weights of K_3^* and K_4^* are increased by a factor of 1.5, leading to a probability of 2%.

As a consistency check of the method, we measure the two-body decay modes ($X_s = K^\pm, K_s^0$), and find 171.0 ± 14.0 and 27.1 ± 5.6 events in on-resonance data for $\eta' K^\pm$ and $\eta' K_s^0$ respectively, and no η' signal events for both channels in off-resonance data, leading to the branching fractions $\mathcal{B}(B^\pm \rightarrow \eta' K^\pm) = (6.9 \pm 0.6(\text{stat})) \times 10^{-5}$ and $\mathcal{B}(B^0 \rightarrow \eta' K^0) = (5.6 \pm 1.2(\text{stat})) \times 10^{-5}$. These values

are fully compatible with what has been measured by recent exclusive analyses [13, 14].

In summary, we have measured the branching fraction, $\mathcal{B}(B \rightarrow \eta' X_s) = (3.9 \pm 0.8(\text{stat}) \pm 0.5(\text{syst}) \pm 0.8(\text{model})) \times 10^{-4}$, for $2.0 < p^*(\eta') < 2.7$ GeV/ c . We have also derived the $m(X_s)$ spectrum and found that the data tends to confirm models predicting a peak at high masses and seems to disfavor predictions based only on the diagram of Fig. 1(a,b) for which $m(X_s)$ peaks near 1.4-1.5 GeV/ c^2 [12].

Among the various theoretical conjectures to explain this production, an $\eta'gg$ coupling due to the QCD anomaly has been widely suggested as a likely explanation. However, the $\eta'gg$ form factor initially proposed [4] is disfavored by recent studies of the inclusive production $\Upsilon(1S) \rightarrow \eta' X$ [15, 16]. A recently updated approach [6] exploiting the same η' gluon anomaly could in principle account for the observed branching fraction and the $m(X_s)$ spectrum.

We are grateful for the excellent luminosity and machine conditions provided by our PEP-II colleagues. The collaborating institutions wish to thank SLAC for its support and kind hospitality. This work is supported by DOE and NSF (USA), NSERC (Canada), IHEP (China), CEA and CNRS-IN2P3 (France), BMBF (Germany), INFN (Italy), NFR (Norway), MIST (Russia), and PPARC (United Kingdom). Individuals have received support from the Swiss NSF, A. P. Sloan Foundation, Research Corporation, and Alexander von Humboldt Foundation.

[†] Also with IFIC, Instituto de Física Corpuscular, CSIC-Universidad de Valencia, Valencia, Spain

[‡] Deceased

- [1] BABAR Collaboration, B. Aubert *et al.*, hep-ex/0310028, submitted to Phys. Rev. D .
- [2] BABAR Collaboration, B. Aubert *et al.*, hep-ex/0308015, hep-ex/0311016.
- [3] CLEO Collaboration, Phys. Rev. Lett. **81**, 1786 (1998).
- [4] D. Atwood and A. Soni, Phys. Lett. B **405**, 150 (1997).
- [5] W.S. Hou and B. Tseng, Phys. Rev. Lett. **80**, 434 (1998).
- [6] H. Fritzsch and Y-F. Zhou, Phys. Rev. D **68**, 034015 (2003). In this paper, the Fermi motion of the b quark is added to a model developed earlier in H. Fritzsch, Phys. Lett. B **415**, 83 (1997). This leads to a X_s spectrum favoring high masses, comparable to the one predicted by the two previous references.
- [7] F. Yuan and K.T. Chao, Phys. Rev. D **56**, 2495 (1997).
- [8] CLEO Collaboration, G.Bonvicini *et al.*, Phys. Rev. D **68**, 011101 (2003).
- [9] BABAR Collaboration, B. Aubert *et al.*, Nucl. Instr. Meth. A **479**, 1 (2002).
- [10] G.C. Fox and S. Wolfram, Phys. Rev. Lett. **41**, 1581 (1978).
- [11] Throughout this paper, whenever a mode is given, the charge conjugate state is also implied.
- [12] A.Datta *et al.*, Phys. Lett. B **419**, 369 (1998).
- [13] BABAR Collaboration, B. Aubert *et al.*, Phys. Rev. Lett. **91**, 161801 (2003).
- [14] Belle Collaboration, K. Abe *et al.*, Phys. Lett. B **517**, 309 (2001).
- [15] A.L. Kagan, AIP Conf. Proc. 618, 310 (2002).
- [16] CLEO Collaboration, M. Artuso *et al.*, Phys. Rev. D **67**, 052003 (2003).

* Also with Università della Basilicata, Potenza, Italy